SECOND-ORDER CONVEX SPLITTING SCHEMES FOR GRADIENT FLOWS WITH EHRLICH-SCHWOEBEL TYPE ENERGY: APPLICATION TO THIN FILM EPITAXY

JIE SHEN
DEPARTMENT OF MATHEMATICS, PURDUE UNIVERSITY
WEST LAFAYETTE, IN 47907-2067
AND
CHENG WANG
DEPARTMENT OF MATHEMATICS, U. MASSACHUSETTS, DARTMOUTH
NORTH DARTMOUTH, MA 02747-2300
AND
XIAOMING WANG*
DEPARTMENT OF MATHEMATICS, FLORIDA STATE UNIVERSITY
TALLAHASSEE, FL 32306-4510
AND
STEVEN M. WISE
DEPARTMENT OF MATHEMATICS, U. OF TENNESSEE
KNOXVILLE, TN 37996-1300

Abstract. We construct unconditionally stable, uniquely solvable and second-order in time schemes for gradient flows with energy of the form $\int_\Omega \left(F(\nabla\phi(\mathbf{x})) + \frac{\epsilon^2}{2}|\Delta\phi(\mathbf{x})|^2 \right) d\mathbf{x}$. The construction of the schemes involves appropriate combination and extensions of two classical ideas: (i) appropriate convex-concave decomposition of the energy functional, and (ii) the secant method. As an application, we derive unconditionally stable, second-order in time schemes for epitaxial growth models with slope selection ($F(\mathbf{y}) = \frac{1}{4}(|\mathbf{y}|^2-1)^2$) or without slope selection ($F(\mathbf{y}) = -\frac{1}{2}\ln(1+|\mathbf{y}|^2)$). Two types of unconditionally stable uniquely solvable second order schemes are presented. The first type inherits the variational structure of the original continuous in time gradient flow while the second type does not preserve the variational structure. We present numerical simulations for the case with slope selection which verify well-known physical scaling laws for the long time coarsening process.

Key words. unconditional stability, second order scheme, convex-concave decomposition, epitaxial growth, Urhlich-Schwoebel type energy

AMS subject classifications. 65M12, 37L65, 65M06, 65M70, 65Z05, 37L15

1. Introduction.

Coarsening, *i.e.*, the process by which a group of objects of different sizes transforms into a group consisting of fewer objects with larger average size, is a very common natural phenomenon and has attracted considerable attention recently [8]. The coarsening process usually takes place on a very long time scale for large systems [9]. Therefore it is important to have accurate and efficient time stepping with regard to numerical simulation.

Many phenomenological macroscopic coarsening processes are energy driven in the sense that the dynamics is the gradient flow of a certain "energy functional" [14, 15]. One well-known example associated with epitaxial thin film growth is the gradient flow with the "energy" taking the form (non-dimensionalized)

$$E(\phi) = \int_\Omega \left(F(\nabla\phi(\mathbf{x})) + \frac{\epsilon^2}{2}|\Delta\phi(\mathbf{x})|^2 \right) d\mathbf{x} \ , \tag{1.1}$$

where $F(\mathbf{y})$ is a smooth function of its argument $\mathbf{y}$, $\Omega = \mathbb{T}^d$ is the domain taken to be the d dimensional periodic box with period 2π and $d = 2, 3, ...$, $\phi : \Omega \to \mathbb{R}$ is a periodic height function (in a moving reference frame) with average zero, and ϵ is a constant (inversely proportional to the size of the system). The first term,

$$E_{ES}(\phi) = \int_\Omega F(\nabla_{\mathbf{x}}\phi(\mathbf{x}))\, d\mathbf{x} \ , \tag{1.2}$$

represents a continuum description of the Ehrlich-Schwoebel effect—according to which adatoms (absorbed atoms) must overcome a higher energy barrier to stick to a step from an upper rather than from a lower

*CORRESPONDING AUTHOR, WXM@MATH.FSU.EDU

terrace [7, 22]—while the second term,

$$E_{SD}(\phi) = \int_\Omega \frac{\epsilon^2}{2} |\Delta\phi(\mathbf{x})|^2 \, d\mathbf{x} \ , \tag{1.3}$$

represents the surface diffusion effect. The case with higher order diffusion as well as Neumann type boundary condition can be considered as well [17].

There are two popular choices for the Ehrlich-Schwoebel energy (1.2). The *case without slope selection*:

$$E_1(\phi) = \int_\Omega \left(-\frac{1}{2} \ln(1 + |\nabla\phi|^2) + \frac{\epsilon^2}{2} |\Delta\phi|^2 \right) d\mathbf{x} \ , \tag{1.4}$$

and the *case with slope selection*:

$$E_2(\phi) = \int_\Omega \left(\frac{1}{4} \Big(|\nabla\phi|^2 - 1 \Big)^2 + \frac{\epsilon^2}{2} |\Delta\phi|^2 \right) d\mathbf{x} \ . \tag{1.5}$$

The second energy may be viewed as an approximation of the first energy under the assumption that the gradient of the height is small [18]. There are significant differences between the two models with the second (simplified) model having a slope selection mechanism (structures with $|\nabla\phi| = 1$ are preferred) that is absent in the first model. This leads to differences in energy minimizers and long time coarsening processes [14, 16, 18].

The variational derivatives of these functionals, which may be interpreted as chemical potentials, can be calculated formally as

$$\mu := \frac{\delta E(\phi)}{\delta\phi} = -\nabla_{\mathbf{x}} \cdot \nabla_{\mathbf{y}} F(\nabla_{\mathbf{x}}\phi) + \epsilon^2 \Delta^2 \phi \ . \tag{1.6}$$

The gradient flow then takes the form

$$\frac{\partial\phi}{\partial t} = -M\mu = M \left(\nabla_{\mathbf{x}} \cdot \nabla_{\mathbf{y}} F(\nabla_{\mathbf{x}}\phi) - \epsilon^2 \Delta^2 \phi \right) \ , \tag{1.7}$$

where $M > 0$ is a mobility, which can be always set to 1 ($M = 1$) by rescaling the time, and periodic boundary conditions are assumed for ϕ in both spatial directions for simplicity.

The physically interesting coarsening process for spatially large systems (small ϵ) occurs on a very long time scale. For instance, for the model with slope selection, the minimal energy is of the order of ϵ [14]. Assuming the widely believed $t^{-\frac{1}{3}}$ scaling for the energy [16, 18, 19], it requires about $\frac{1}{\epsilon^3}$ time for the system to reach saturation from an initially order one profile (the saturation time would be of the order of ϵ^{-2} under the scaling that we have adopted for our equation). Therefore, numerical simulations for the coarsening process of large systems require long time accuracy and stability. In particular, higher order (with respect to time discretization) schemes are very desirable. In addition, unconditional energy stability is also coveted, since we would like to have the capability of preserving the stability even if we take large time step (in adaptive time stepping for instance).

Various first-order unconditionally energy stable schemes for models of thin film epitaxial growth are derived recently [3, 28]. The purpose of this manuscript is to construct convex splitting schemes that are second-order in time, uniquely solvable and unconditionally energy stable for gradient flows with Ehrlich-Schwoebel type energy and apply them to models of thin film epitaxy. We note that second-order, uniquely solvable, and unconditionally energy stable schemes have been constructed recently in [29] for Swift-Hohenberg and phase field crystal type equations. The schemes in [29] can be applied to Allen-Cahn and Cahn-Hilliard-type equations, as well as other gradient flows where the nonlinearity involves only the height function. (We refer to [5, 23, 24, 31, 4, 27] for other related convexity splitting schemes.) It is not obvious whether any of the schemes from the works just mentioned can be extended to gradient flows with an Ehrlich-Schwoebel type energy that is a function of the gradient of the height function (instead of the height function only). We also

point out that efficient second and third order in time accurate schemes have been investigated in [30] with energy stability verified under certain assumptions on the numerically computed solutions.

The rest of the paper is organized as follows. In section 2 we present and analyze a family of second order in time, uniquely solvable, unconditionally energy stable schemes that preserves the variational structure of the continuous in time model. We introduce alternative schemes with all the desired properties except the variational structure in section 3. Section 4 is devoted to specific applications to the models of thin film epitaxial growth with or without slope selection. Fully discretized schemes including Galerkin Fourier-spectral, collocation Fourier-spectral and finite-difference in space are considered in section 5. Numerical results based on finite-difference in space and time stepping proposed in section 2 applied to the case with slope selection is presented in section 6. We offer our conclusion remarks in section 7.

2. The scheme with variational structure. Without loss of generality, we assume that the Ehrlich-Schwoebel type energy density $F(\mathbf{y})$ is smooth and possesses a convex (+) – concave (-) splitting with a quadratic concave term, *i.e.*,

$$F(\mathbf{y}) = F_+(\mathbf{y}) + F_-(\mathbf{y}) \quad \text{with} \quad F_-(\mathbf{y}) = -C|\mathbf{y}|^2 \ . \tag{2.1}$$

The philosophy we shall use to construct a second-order energy stable scheme is a combination of the convex-concave splitting (see [11] for instance) and the secant method (see for instance [5]) modified so that it can be applied to vector form and utilized on the convex part only.

Following the general idea of treating the convex part implicitly and the concave part explicitly, a second-order convex splitting scheme should take the following form for the gradient flow (1.7)

$$\begin{aligned} &\frac{\phi^{n+1}-\phi^n}{k}+\frac{\epsilon^2}{2}\Delta^2(\phi^{n+1}+\phi^n)+\nabla_{\mathbf{x}}\cdot H_n^{n+1}(F_+) \\ &\qquad = \nabla_{\mathbf{x}}\cdot\left(\frac{3}{2}\nabla_{\mathbf{y}}F_-(\nabla_{\mathbf{x}}\phi^n)-\frac{1}{2}\nabla_{\mathbf{y}}F_-(\nabla_{\mathbf{x}}\phi^{n-1})\right) \end{aligned} \tag{2.2}$$

where $H_n^{n+1}(F_+)$ should be chosen such that the above scheme is second-order at $t_{n+\frac{1}{2}}$ and energy stable. Since the energy stability is usually proved by taking the inner product of the above with $(\phi^{n+1}-\phi^n)$, the following inequality has to be satisfied:

$$(H_n^{n+1}(F_+), \nabla(\phi^{n+1}-\phi^n)) \geq \int_\Omega F_+(\nabla\phi^{n+1})\,d\mathbf{x} - \int_\Omega F_+(\nabla\phi^n)\,d\mathbf{x}. \tag{2.3}$$

By direct calculation, we have

$$\begin{aligned} &\int_\Omega F_+(\nabla\phi^{n+1})\,d\mathbf{x} - \int_\Omega F_+(\nabla\phi^n)\,d\mathbf{x} \\ &\quad = \int_\Omega\int_0^1 \frac{d}{d\tau}F_+(\mathbf{y}_0+\tau(\mathbf{y}-\mathbf{y}_0))\,d\tau\Big|_{\mathbf{y}=\nabla_{\mathbf{x}}\phi^{n+1},\mathbf{y}_0=\nabla_{\mathbf{x}}\phi^n} d\mathbf{x} \\ &\quad = \int_\Omega\int_0^1 (\nabla_{\mathbf{y}}F_+(\mathbf{y}))\Big|_{\mathbf{y}=\nabla_{\mathbf{x}}\phi^n+\tau(\nabla_{\mathbf{x}}\phi^{n+1}-\nabla_{\mathbf{x}}\phi^n)} d\tau\cdot(\nabla_{\mathbf{x}}\phi^{n+1}-\nabla_{\mathbf{x}}\phi^n)\,d\mathbf{x} \\ &\quad = -\int_\Omega \nabla_{\mathbf{x}}\cdot\left(\int_0^1 (\nabla_{\mathbf{y}}F_+(\mathbf{y}))\Big|_{\mathbf{y}=\nabla_{\mathbf{x}}\phi^n+\tau(\nabla_{\mathbf{x}}\phi^{n+1}-\nabla_{\mathbf{x}}\phi^n)} d\tau\right)(\phi^{n+1}-\phi^n)\,d\mathbf{x}. \end{aligned} \tag{2.4}$$

Therefore, a natural choice for H_n^{n+1} is

$$H_n^{n+1}(F_+) = -\nabla_{\mathbf{x}}\cdot\left(\int_0^1 (\nabla_{\mathbf{y}}F_+(\mathbf{y}))\Big|_{\mathbf{y}=\nabla_{\mathbf{x}}\phi^n+\tau(\nabla_{\mathbf{x}}\phi^{n+1}-\nabla_{\mathbf{x}}\phi^n)} d\tau\right), \tag{2.5}$$

and our second-order convex splitting scheme is:

$$\frac{\phi^{n+1}-\phi^n}{k}+\frac{\epsilon^2}{2}\Delta^2(\phi^{n+1}+\phi^n)-\nabla_{\mathbf{x}}\cdot\left(\int_0^1(\nabla_{\mathbf{y}}F_+(\mathbf{y}))\Big|_{\mathbf{y}=\nabla_{\mathbf{x}}\phi^n+\tau(\nabla_{\mathbf{x}}\phi^{n+1}-\nabla_{\mathbf{x}}\phi^n)}d\tau\right)$$
$$=\nabla_{\mathbf{x}}\cdot\left(\frac{3}{2}\nabla_{\mathbf{y}}F_-(\nabla_{\mathbf{x}}\phi^n)-\frac{1}{2}\nabla_{\mathbf{y}}F_-(\nabla_{\mathbf{x}}\phi^{n-1})\right). \tag{2.6}$$

Alternatively, we can write the above scheme in the weak form: find $\phi^{n+1}\in\dot{H}^2_{per}(\Omega):=\{\phi\in H^2(\Omega):\ \phi$ is periodic with average zero$\}$ such that

$$\left(\frac{\phi^{n+1}-\phi^n}{k},\psi\right)+\left(\frac{\epsilon^2}{2}\Delta(\phi^{n+1}+\phi^n),\Delta\psi\right)+\left(\int_0^1(\nabla_{\mathbf{y}}F_+(\mathbf{y}))\Big|_{\mathbf{y}=\nabla_{\mathbf{x}}\phi^n+\tau(\nabla_{\mathbf{x}}\phi^{n+1}-\nabla_{\mathbf{x}}\phi^n)}d\tau,\nabla_{\mathbf{x}}\psi\right)$$
$$=\left(\frac{3}{2}\nabla_{\mathbf{y}}F_-(\nabla_{\mathbf{x}}\phi^n)-\frac{1}{2}\nabla_{\mathbf{y}}F_-(\nabla_{\mathbf{x}}\phi^{n-1}),\nabla_{\mathbf{x}}\psi\right),\quad\forall\psi\in\dot{H}^2_{per}(\Omega). \tag{2.7}$$

Note that the treatment of the concave part is unique in the sense that, for quadratic energy, this is the only way to get second-order with explict two-step treatment. The treatment of the diffusion term is not unique. We have utilized the midpoint rule corresponding to Crank-Nicolson approach. Alternative approximations, such as $\frac{3}{4}\Delta^2\phi^{n+1}+\frac{1}{4}\Delta^2\phi^{n-1}$, can be used as well if more dissipation is desired.

The main result of this section is the following

Theorem 1. *Under the assumption* (2.1)*, the scheme* (2.7) *is second-order accurate in time and unconditionally stable. More precisely, we have*

$$E(\phi^{n+1})+\frac{C}{2}\|\nabla(\phi^{n+1}-\phi^n)\|^2+\frac{\|\phi^{n+1}-\phi^n\|^2}{k}+\frac{C}{2}\|\nabla(\phi^{n+1}+\phi^{n-1}-2\phi^n)\|^2$$
$$=E(\phi^n)+\frac{C}{2}\|\nabla(\phi^n-\phi^{n-1})\|^2\ . \tag{2.8}$$

Moreover, at each time step, the scheme corresponds to the Euler-Lagrange equation for the following strictly convex coercive variation problem:

$$E_{scheme}(\phi,\phi^n,\phi^{n-1})=\frac{\epsilon^2}{2}\|\Delta\phi\|^2+\frac{1}{2k}\|\phi\|^2+\int_\Omega\mathcal{F}_p(\nabla\phi,\nabla\phi^n)\,d\mathbf{x}$$
$$+\int_\Omega\left(-\nabla\cdot(\frac{3}{2}\nabla_{\mathbf{y}}F_-(\nabla\phi^n)-\frac{1}{2}\nabla_{\mathbf{y}}F_-(\nabla\phi^{n-1}))\right.$$
$$\left.+\frac{\epsilon^2}{2}\Delta^2\phi^n-\frac{\phi^n}{k}\right)\phi\,d\mathbf{x} \tag{2.9}$$

with

$$\mathcal{F}_p(\nabla\phi,\nabla\phi^n)=\int_0^1\frac{1}{\tau}\left(F_+(\nabla\phi^n+\tau(\nabla\phi-\nabla\phi^n))-F_+(\nabla\phi^n)\right)d\tau. \tag{2.10}$$

Therefore, the scheme is uniquely solvable provided that $F_+(\mathbf{y})$ and $\nabla_{\mathbf{y}}F_+(\mathbf{y})$ grow at most like a polynomial in $\mathbf{y}$.

Proof. By taking the Taylor expansion at $t_{n+\frac{1}{2}}$, it is easy to see that the scheme is second-order accurate in time.

The unconditional stability of the scheme is guaranteed by the discrete energy law (2.8). In order to derive this discrete energy law, we take $\psi=\phi^{n+1}-\phi^n$ in (2.7).

Obviously, we have

$$\int_\Omega-\frac{\epsilon^2}{2}\Delta^2(\phi^{n+1}+\phi^n)(\phi^{n+1}-\phi^n)\,d\mathbf{x}=-\frac{\epsilon^2}{2}\int_\Omega(|\Delta\phi^{n+1}|^2-|\Delta\phi^n|^2)\,d\mathbf{x}. \tag{2.11}$$

Thanks to the assumption (2.1), we have $\nabla_{\mathbf{y}} F_-(\mathbf{y}) = -2C\mathbf{y}$. Therefore,

$$
\begin{aligned}
&-\int_\Omega \left(\frac{3}{2}\nabla_{\mathbf{y}} F_-(\nabla_{\mathbf{x}}\phi^n) - \frac{1}{2}\nabla_{\mathbf{y}} F_-(\nabla_{\mathbf{x}}\phi^{n-1})\right)\cdot\nabla_{\mathbf{x}}(\phi^{n+1}-\phi^n)\,d\mathbf{x}\\
&\quad = C\int_\Omega (3\nabla\phi^n - \nabla\phi^{n-1})\cdot(\nabla\phi^{n+1}-\nabla\phi^n)\,d\mathbf{x}\\
&\quad = 2C\int_\Omega \nabla\phi^n\cdot(\nabla\phi^{n+1}-\nabla\phi^n)\,d\mathbf{x} + C\int_\Omega (\nabla\phi^n-\nabla\phi^{n-1})\cdot(\nabla\phi^{n+1}-\nabla\phi^n)\,d\mathbf{x}\\
&\quad = C\int_\Omega \left(-|\nabla\phi^n|^2 + |\nabla\phi^{n+1}|^2 - |\nabla(\phi^{n+1}-\phi^n)|^2 + (\nabla\phi^n-\nabla\phi^{n-1})\cdot(\nabla\phi^{n+1}-\nabla\phi^n)\right)\,d\mathbf{x}\\
&\quad = C\int_\Omega \left(-|\nabla\phi^n|^2 + |\nabla\phi^{n+1}|^2 - \frac{1}{2}|\nabla(\phi^{n+1}-\phi^n)|^2 + \frac{1}{2}|\nabla\phi^n-\nabla\phi^{n-1}|^2\right)\\
&\qquad -C\int_\Omega \frac{1}{2}|\nabla(\phi^{n+1}+\phi^{n-1}-2\phi^n)|^2\,d\mathbf{x}\,. \qquad (2.12)
\end{aligned}
$$

Combining the above two inequalities and (2.4), we deduce the desired discrete energy law (2.8).
On the other hand, we can easily verify that

$$
\nabla_{\mathbf{x}}\cdot\left(\int_0^1 (\nabla_{\mathbf{y}} F_+(\mathbf{y}))\Big|_{\mathbf{y}=\nabla_{\mathbf{x}}\phi^n+\tau(\nabla_{\mathbf{x}}\phi^{n+1}-\nabla_{\mathbf{x}}\phi^n)}\,d\tau\right) = -\frac{\delta\int_\Omega \mathcal{F}_p(\nabla\phi^{n+1},\nabla\phi^n)\,d\mathbf{x}}{\delta\phi^{n+1}}\,. \qquad (2.13)
$$

Therefore the scheme (2.6) is the Euler-Lagrange equation of the energy functional given in (2.9). The convexity of $\mathcal{F}_p$ follows from the convexity of

$$
\frac{1}{\tau}\left(F_+(\nabla\phi^n+\tau(\nabla\phi-\nabla\phi^n)) - F_+(\nabla\phi^n)\right)
$$

for all $\tau\in(0,1]$, thanks to the convexity of F_+. So the coercivity of the energy functional (2.9) then follows from the convexity of $\mathcal{F}_p$ and the diffusion term. Therefore, the unique solution to the scheme exists and is the unique minimizer of the energy functional (2.9) under usual differentiability and growth conditions on F_+ [6, 10, 12]. □

3. Alternative schemes without variational structure. Alternative second-order unconditionally stable and uniquely solvable schemes do exist if we do not care about the preservation of the variational structure. In this case, straightforward generalization of the secant method would work without involving the integral form that we used in deriving the scheme with variational structure that we presented in the previous section. The resulting schemes are generally more compact than the schemes derived in the previous section although they lack the variational structure. Here we illustrate two alternative ways of deriving second-order unconditionally stable and uniquely solvable schemes for equations of thin film epitaxial growth with or without slope selection.

Without loss of generality, we assume that the Ehrlich-Schwoebel type energy density $F(\mathbf{y})$ is smooth and takes the form

$$
F(\mathbf{y}) = G(|\mathbf{y}|^2). \qquad (3.1)
$$

This certainly fits the thin film epitaxy models that we are interested here with $G(\xi) = -\frac{1}{2}\ln(1+\xi)$ for the case without slope selection, and $G(\xi) = \frac{1}{4}(\xi-1)^2$ for the case with slope selection.

Following the general convex-splitting idea (see for instance [11, 28]), we assume that it possesses a convex-concave splitting with a quadratic concave term, *i.e.*,

$$
G(\xi) = G_+(\xi) + G_-(\xi) \quad \text{with} \quad G_+'' \ge 0, \quad G_+' \ge 0 \quad \text{and} \quad G_-(\xi) = -C\xi. \qquad (3.2)
$$

We now construct a scheme with the following considerations: (i) The concave quadratic term associated with G_- can be treated explicitly via classical two level method as before in order to preserve the energy

law and maintain the second-order accuracy; (ii) Likewise, the convex quadratic term ($\frac{\epsilon^2}{2}\|\Delta\phi|^2$) can be treated easily using classical midpoint type approximation; (iii) For the convex part associated with G_+, we mimic the classical secant method for second-order approximation (see for instance [5]) in this vector setting. Taking into accounts the above considerations, we arrive at the following second-order scheme

$$\begin{aligned}\frac{\phi^{n+1}-\phi^n}{k} &= \nabla\cdot\left(\frac{G_+(|\nabla\phi^{n+1}|^2)-G_+(|\nabla\phi^n|^2)}{|\nabla\phi^{n+1}|^2-|\nabla\phi^n|^2}(\nabla\phi^{n+1}+\nabla\phi^n)\right)\\ &\quad+\nabla\cdot\left(3G'_-(|\nabla\phi^n|^2)\nabla\phi^n-G'_-(|\nabla_{\mathbf{x}}\phi^{n-1}|^2)\nabla\phi^{n-1}\right)-\frac{\epsilon^2}{2}\Delta^2(\phi^{n+1}+\phi^n)\ .\end{aligned}\tag{3.3}$$

The weak form of the above scheme is: find $\phi^{n+1}\in\dot{H}^2_{per}(\Omega)$ such that

$$\begin{aligned}&\left(\frac{\phi^{n+1}-\phi^n}{k},\psi\right)+\left(\frac{\epsilon^2}{2}\Delta(\phi^{n+1}+\phi^n),\Delta\psi\right)+\left(\frac{G_+(|\nabla\phi^{n+1}|^2)-G_+(|\nabla\phi^n|^2)}{|\nabla\phi^{n+1}|^2-|\nabla\phi^n|^2}(\nabla\phi^{n+1}+\nabla\phi^n),\nabla\psi\right)\\ &\qquad=\left(3G'_-(|\nabla\phi^n|^2)\nabla\phi^n-G'_-(|\nabla_{\mathbf{x}}\phi^{n-1}|^2)\nabla\phi^{n-1},\nabla\psi\right),\quad\forall\psi\in\dot{H}^2_{per}(\Omega).\end{aligned}\tag{3.4}$$

Theorem 2. *Under the assumption* (3.2)*, the alternative scheme (3.3) is second-order accurate in time, unconditionally energy stable in the sense that*

$$\begin{aligned}E(\phi^{n+1})+\frac{C}{2}\|\nabla(\phi^{n+1}-\phi^n)\|^2+\frac{\|\phi^{n+1}-\phi^n\|^2}{k}+\frac{C}{2}\|\nabla(\phi^{n+1}+\phi^{n-1}-2\phi^n)\|^2\\ =E(\phi^n)+\frac{C}{2}\|\nabla(\phi^n-\phi^{n-1})\|^2.\end{aligned}\tag{3.5}$$

Moreover, for the case energy functional given by the model with slope selection (1.5)*, and with the splitting given by $G_+(\xi)=\frac{1}{4}\xi^2+\frac{1}{4}, G_-(\xi)=-\frac{1}{2}\xi$, the scheme is uniquely solvable.*

Proof. The second-order accuracy of this scheme (3.4) can be verified by taking the Taylor expansion at $t_{n+\frac{1}{2}}$.

In order to prove the energy law (3.5), we take $\psi=\phi^{n+1}-\phi^n$ in (3.4). Notice that with the assumption (3.2), the contribution of the concave part is exactly the same as in (2.12). Thus, the energy law (3.5) follows similarly.

To prove the unique solvability, we need the following lemma.

Lemma 1. *Consider the (nonlinear) problem*

$$\frac{\phi}{k}-\nabla\cdot\mathcal{F}(\nabla\phi,\mathbf{x})+\frac{\epsilon^2}{2}\Delta^2\phi=f\tag{3.6}$$

where $\mathcal{F}, f$ are given (smooth) functions. Then a sufficient condition on uniqueness (of sufficiently smooth solution) is that the symmetric part of the Jacobian of $\mathcal{F}$ is non-negative.

Proof of the lemma: Suppose we have two solutions $\phi,\tilde{\phi}$ to the general scheme (3.6). Then, we have

$$\frac{\phi-\tilde{\phi}}{k}-\nabla\cdot(\mathcal{F}(\nabla\phi,\mathbf{x})-\mathcal{F}(\nabla\tilde{\phi},\mathbf{x}))+\frac{\epsilon^2}{2}\Delta^2(\phi-\tilde{\phi})=0.$$

Taking the inner product of this equation with $\phi-\tilde{\phi}$, we deduce

$$\begin{aligned}0&=\frac{\|\phi-\tilde{\phi}\|^2}{k}+\int_\Omega(\mathcal{F}(\nabla\phi,\mathbf{x})-\mathcal{F}(\nabla\tilde{\phi},\mathbf{x}))\cdot\nabla(\phi-\tilde{\phi})\,d\mathbf{x}+\frac{\epsilon^2}{2}\|\Delta(\phi-\tilde{\phi})\|^2\\ &=\frac{\|\phi-\tilde{\phi}\|^2}{k}+\int_\Omega\int_0^1(J(\mathcal{F})(\nabla\tilde{\phi}+\tau\nabla(\phi-\tilde{\phi}),\mathbf{x})\nabla(\phi-\tilde{\phi}))\,d\tau\cdot\nabla(\phi-\tilde{\phi})\,d\mathbf{x}+\frac{\epsilon^2}{2}\|\Delta(\phi-\tilde{\phi})\|^2\\ &\geq\frac{\|\phi-\tilde{\phi}\|^2}{k}+\frac{\epsilon^2}{2}\|\Delta(\phi-\tilde{\phi})\|^2,\end{aligned}$$

where in the last step we have used the assumption that the symmetric part of the Jacobian of $\mathcal{F}$ is non-negative. □

It is now straightforward to prove the unique solvability stated in the theorem. Indeed, with the specific choice of G_+ and G_-, we have

$$\begin{aligned} J(\mathcal{F}(\mathbf{y})) &= \int_0^1 \int_0^s G_+''(|\mathbf{y}|^2 + \tau(|\mathbf{y}_0|^2 - |\mathbf{y}|^2))[|\mathbf{y}_0|^2 - |\mathbf{y}|^2 + 2\mathbf{y} \otimes (\mathbf{y} + \mathbf{y}_0)]\, d\tau ds + G'(|\mathbf{y}|^2) I \\ &= \frac{1}{4}\left((|\mathbf{y}_0|^2 + |\mathbf{y}|^2) I + (\mathbf{y} + \mathbf{y}_0) \otimes (\mathbf{y} + \mathbf{y}_0) + \mathbf{y} \otimes \mathbf{y} - \mathbf{y}_0 \otimes \mathbf{y}_0 + (\mathbf{y} \otimes \mathbf{y}_0 - \mathbf{y}_0 \otimes \mathbf{y})\right). \end{aligned}$$

It is then easy to observe that the symmetric part of this Jacobian matrix is non-negative.

Notice that this Jacobian matrix is non-symmetric in general. Therefore, we can conclude that the term $\nabla_{\mathbf{x}} \mathcal{F}(\nabla \phi^{n+1})$ can not be interpreted as the variational derivative of any energy functional of $\nabla \phi^{n+1}$ since that would imply the symmetry of the Jacobian. □

The scheme (3.3), while being more compact than the scheme (2.6), is only guaranteed to be uniquely solvable for the energy with slope selection (1.5). At the expense of compactness we can construct second-order unconditionally stable, uniquely solvable scheme for more general energy functional. In this case, we adapt the classical secant method for the convex term to our vector setting via splitting the direction and a symmetrisation at the end. In the two-dimensional case, the scheme takes the following form:

$$\begin{aligned} \frac{\phi^{n+1} - \phi^n}{k} = \partial_{x_1} & \frac{F_+(\nabla \phi^{n+1}) - F_+(\psi^*) + F_+(\psi_*) - F_+(\nabla \phi^n)}{\partial_{x_1}(\phi^{n+1} - \phi^n)} \\ & + \partial_{x_2} \frac{F_+(\nabla \phi^{n+1}) - F_+(\psi_*) + F_+(\psi^*) - F_+(\nabla \phi^n)}{\partial_{x_2}(\phi^{n+1} - \phi^n)} \\ & + \nabla_{\mathbf{x}} \cdot \left(\frac{3}{2} \nabla_{\mathbf{y}} F_-(\nabla_{\mathbf{x}} \phi^n) - \frac{1}{2} \nabla_{\mathbf{y}} F_-(\nabla_{\mathbf{x}} \phi^{n-1}) \right) - \frac{\epsilon^2}{2} \Delta^2 (\phi^{n+1} + \phi^n) \end{aligned} \tag{3.7}$$

where

$$\psi^* = (\partial_{x_1} \phi^n, \partial_{x_2} \phi^{n+1}), \psi_*(\partial_{x_1} \phi^{n+1}, \partial_{x_2} \phi^n).$$

The scheme for the three-dimensional case can be constructed accordingly.

It is straightforward to verify that this scheme is second-order accurate, unconditionally stable and uniquely solvable with the convex-concave decomposition as before. It can also be verified that the scheme (3.7) coincides with the scheme (3.3) for the model with slope selection using the convex-concave splitting given in (4.1). Therefore, this scheme does not possesses variational structure either. We leave the detail to the interested reader.

4. Application to thin film epitaxy.

4.1. Case with slope selection. In this case, a convenient splitting of the Ehrlich-Schwoebel energy density $F(\mathbf{y}) = \frac{1}{4}(|\mathbf{y}|^2 - 1)^2$ is

$$F_+(\mathbf{y}) = \frac{1}{4}|\mathbf{y}|^4 + \frac{1}{4}, \quad F_-(\mathbf{y}) = -\frac{1}{2}|\mathbf{y}|^2 \ . \tag{4.1}$$

In this case we can calculate the (variational) potential defined in (2.10) associated with the convex part

of the scheme as

$$\begin{aligned}
&\mathcal{F}_p(\mathbf{y},\mathbf{y}_0) = \int_0^1 \frac{1}{4\tau}(|\mathbf{y}_0+\tau(\mathbf{y}-\mathbf{y}_0)|^4 - |\mathbf{y}_0|^4)\,d\tau \\
&= \int_0^1 \frac{1}{4}(|\mathbf{y}_0+\tau(\mathbf{y}-\mathbf{y}_0)|^2 + |\mathbf{y}_0|^2)(2\mathbf{y}_0+\tau(\mathbf{y}-\mathbf{y}_0))\cdot(\mathbf{y}-\mathbf{y}_0)\,d\tau \\
&= \int_0^1 \frac{1}{4}(2|\mathbf{y}_0|^2 + 2\tau\mathbf{y}_0\cdot(\mathbf{y}-\mathbf{y}_0) + \tau^2|\mathbf{y}-\mathbf{y}_0|^2)(2\mathbf{y}_0\cdot(\mathbf{y}-\mathbf{y}_0)+\tau|\mathbf{y}-\mathbf{y}_0|^2)\,d\tau \\
&= \frac{1}{4}(4\mathbf{y}_0\cdot(\mathbf{y}-\mathbf{y}_0)|\mathbf{y}_0|^2 + 2(\mathbf{y}_0\cdot(\mathbf{y}-\mathbf{y}_0))^2 + \frac{4}{3}\mathbf{y}_0\cdot(\mathbf{y}-\mathbf{y}_0)|\mathbf{y}-\mathbf{y}_0|^2 + |\mathbf{y}_0|^2|\mathbf{y}-\mathbf{y}_0|^2 + \frac{1}{4}|\mathbf{y}-\mathbf{y}_0|^4) \\
&= \frac{1}{4}(\frac{1}{4}|\mathbf{y}|^4 + \frac{1}{3}\mathbf{y}_0\cdot\mathbf{y}|\mathbf{y}|^2 + \frac{1}{6}|\mathbf{y}_0|^2|\mathbf{y}|^2 + \frac{1}{3}(\mathbf{y}_0\cdot\mathbf{y})^2 + \mathbf{y}_0\cdot\mathbf{y}|\mathbf{y}_0|^2 - \frac{25}{12}|\mathbf{y}_0|^4). \qquad (4.2)
\end{aligned}$$

Therefore

$$\frac{\delta\mathcal{F}_p}{\delta\mathbf{y}} = \frac{1}{4}(|\mathbf{y}|^2\mathbf{y} + |\mathbf{y}_0|^2\mathbf{y}_0) + \frac{1}{12}(|\mathbf{y}|^2\mathbf{y}_0 + |\mathbf{y}_0|^2\mathbf{y} + 2(\mathbf{y}_0\cdot\mathbf{y})(\mathbf{y}+\mathbf{y}_0)). \qquad (4.3)$$

Thanks to (2.13), the scheme (2.6) becomes

$$\begin{aligned}
\frac{\phi^{n+1}-\phi^n}{k} = &\frac{1}{4}\nabla\cdot(|\nabla\phi^{n+1}|^2\nabla\phi^{n+1} + |\nabla\phi^n|^2\nabla\phi^n) \\
&+\frac{1}{12}\nabla\cdot(|\nabla\phi^{n+1}|^2\nabla\phi^n + |\nabla\phi^n|^2\nabla\phi^{n+1} + 2(\nabla\phi^n\cdot\nabla\phi^{n+1})(\nabla\phi^n+\nabla\phi^{n+1})) \\
&-\Delta(\frac{3}{2}\phi^n - \frac{1}{2}\phi^{n-1}) - \frac{\epsilon^2}{2}\Delta^2(\phi^{n+1}+\phi^n)\ . \qquad (4.4)
\end{aligned}$$

On the other hand, it is easy to check that in this case, the scheme (3.3) and the scheme (3.7) takes the form

$$\begin{aligned}
\frac{\phi^{n+1}-\phi^n}{k} = &\frac{1}{4}\nabla\cdot[(|\nabla\phi^{n+1}|^2 + |\nabla\phi^n|^2)(\nabla\phi^{n+1}+\nabla\phi^n)] \\
&-\Delta(\frac{3}{2}\phi^n - \frac{1}{2}\phi^{n-1}) - \frac{\epsilon^2}{2}\Delta^2(\phi^{n+1}+\phi^n)\ . \qquad (4.5)
\end{aligned}$$

Note that the above scheme is more compact than the scheme (4.4). In fact, the scheme (4.4) may be viewed as the symmetrization of the scheme (4.5).

4.2. Case without slope selection. In this case, a convenient convex-concave splitting of the Ehrlich-Schwoebel energy density $F(\mathbf{y}) = -\frac{1}{2}\ln(1+|\mathbf{y}|^2)$ is ([28])

$$F_+(\mathbf{y}) = |\mathbf{y}|^2 - \frac{1}{2}\ln(1+|\mathbf{y}|^2)\ , \quad F_-(\mathbf{y}) = -|\mathbf{y}|^2\ . \qquad (4.6)$$

It seems non-trivial to represent the (variational) potential $\mathcal{F}_p$ associated with the convex part using elementary functions. However, we note that only the variational derivative is needed in the weak form of

the scheme (2.7), and it can be calculated explicitly as follows:

$$\begin{aligned}
&\int_0^1 (\nabla_{\mathbf{y}} F_+)(\mathbf{y}_0+\tau(\mathbf{y}-\mathbf{y}_0))\,d\tau\\
&=\int_0^1 (2(\mathbf{y}_0+\tau(\mathbf{y}-\mathbf{y}_0))-\frac{\mathbf{y}_0+\tau(\mathbf{y}-\mathbf{y}_0)}{1+|\mathbf{y}_0+\tau(\mathbf{y}-\mathbf{y}_0)|^2})\,d\tau\\
&=2\mathbf{y}_0+(\mathbf{y}-\mathbf{y}_0)-\int_0^1 \frac{\mathbf{y}_0+\tau(\mathbf{y}-\mathbf{y}_0)}{1+|\mathbf{y}_0+\tau(\mathbf{y}-\mathbf{y}_0)|^2}\,d\tau\\
&=2\mathbf{y}_0+(\mathbf{y}-\mathbf{y}_0)-\frac{\mathbf{y}-\mathbf{y}_0}{2|\mathbf{y}-\mathbf{y}_0|}\ln\frac{(1+|\mathbf{y}_0|^2-\frac{(\mathbf{y}_0\cdot(\mathbf{y}-\mathbf{y}_0))^2}{|\mathbf{y}-\mathbf{y}_0|^2})^2+(|\mathbf{y}-\mathbf{y}_0|+\frac{\mathbf{y}_0\cdot(\mathbf{y}-\mathbf{y}_0)}{|\mathbf{y}-\mathbf{y}_0|})^2}{(1+|\mathbf{y}_0|^2-\frac{(\mathbf{y}_0\cdot(\mathbf{y}-\mathbf{y}_0)}{|\mathbf{y}-\mathbf{y}_0|})^2+(\frac{\mathbf{y}_0\cdot(\mathbf{y}-\mathbf{y}_0)}{|\mathbf{y}-\mathbf{y}_0|})^2}\\
&\quad-\frac{\mathbf{y}_0|\mathbf{y}-\mathbf{y}_0|-(\mathbf{y}-\mathbf{y}_0)\frac{\mathbf{y}_0\cdot(\mathbf{y}-\mathbf{y}_0)}{|\mathbf{y}-\mathbf{y}_0|}}{(1+|\mathbf{y}_0|^2)|\mathbf{y}-\mathbf{y}_0|^2-(\mathbf{y}_0\cdot(\mathbf{y}-\mathbf{y}_0))^2}(\tan^{-1}\frac{\frac{\mathbf{y}_0\cdot(\mathbf{y}-\mathbf{y}_0)}{|\mathbf{y}-\mathbf{y}_0|}+|\mathbf{y}-\mathbf{y}_0|}{1+|\mathbf{y}_0|^2-\frac{(\mathbf{y}_0\cdot(\mathbf{y}-\mathbf{y}_0))^2}{|\mathbf{y}-\mathbf{y}_0|^2}}-\tan^{-1}\frac{\frac{\mathbf{y}_0\cdot(\mathbf{y}-\mathbf{y}_0)}{|\mathbf{y}-\mathbf{y}_0|}}{1+|\mathbf{y}_0|^2-\frac{(\mathbf{y}_0\cdot(\mathbf{y}-\mathbf{y}_0))^2}{|\mathbf{y}-\mathbf{y}_0|^2}}),
\end{aligned}\tag{4.7}$$

where in the last step we have utilized the following elementary calculus identity

$$\int \frac{c_1+c_2\tau}{c_3^2+(c_4+c_5\tau)^2}\,d\tau=\frac{c_2}{2c_5}\ln(c_3^2+(c_4+c_5\tau)^2)+\frac{c_1c_5-c_2c_4}{c_3c_5^2}\arctan\frac{c_4+c_5\tau}{c_3}$$

with $c_1=\mathbf{y}_0, c_2=\mathbf{y}-\mathbf{y}_0, c_5=|\mathbf{y}-\mathbf{y}_0|, c_4=\frac{\mathbf{y}_0\cdot(\mathbf{y}-\mathbf{y}_0)}{|\mathbf{y}-\mathbf{y}_0|}, c_3=1+|\mathbf{y}_0|^2-\frac{(\mathbf{y}_0\cdot(\mathbf{y}-\mathbf{y}_0))^2}{|\mathbf{y}-\mathbf{y}_0|^2}$.

This scheme enjoys the nice property of unqiue solvability and variational structure in any dimension on top of the 2nd order accuracy and unconditional energy stability at the expense of compactness. On the other hand, it is straightforward to write down the explicit form for the scheme (3.7) which works in 2D although without the variational structure.

5. Full discretizations.

5.1. Full discretization by a Galerkin method. Notice that the proof of Theorem 1 (resp. Theorem 2) is based on the weak forms (2.7) (resp. (3.4)). Therefore, the results of Theorem 1 (resp. Theorem 2) can be straightforwardly extended to for any consistent Galerkin approximation, such as Fourier-Galerkin method and finite element Galerkin method, of the semi-discrete scheme (2.7) (resp. (3.4)). The only modification needed is to view the "energy" as defined on the finite dimensional Galerkin space, compute the variational derivatives within the same Galerkin projected space, and view the fully discrete scheme as time discretization of a gradient flow on the finite dimensional Galerkin projected space.

5.2. Fourier-Galerkin method with numerical integration. While the results of Theorems 1 (resp. Theorem 2) hold for Fourier-Galerkin approximation to (2.7) (resp. (3.4)), it is usually not practical to implement a pure Fourier-Galerkin method due to the convolution involved in computing nonlinear terms. A common practice is to replace the integral by a numerical quadrature, leading to the so called Fourier-Galerkin method with numerical integration.

We now sketch some detail for the Fourier-Galerkin method with numerical integration. For the sake of simplicity, we shall only consider the alternative scheme for the case with slope selection, namely the scheme (4.5). The Fourier-Galerkin method with numerical integration for other schemes can be formulated in a similar fashion. Let us first write the scheme (4.5) in the following weak form: Find $\phi^{n+1}\in H^2_{p,0}(\Omega)$ such that

$$\begin{aligned}
\left(\frac{\phi^{n+1}-\phi^n}{k},\psi\right)=&-\frac{1}{4}\left((|\nabla\phi^{n+1}|^2+|\nabla\phi^n|^2)(\nabla\phi^{n+1}+\nabla\phi^n),\nabla\psi\right)\\
&+(\nabla(\frac{3}{2}\phi^n-\frac{1}{2}\phi^{n-1}),\nabla\psi)-\frac{\epsilon^2}{2}(\Delta(\phi^{n+1}+\phi^n),\Delta\psi)\ ,\quad \forall\psi\in H^2_{p,0}(\Omega).
\end{aligned}\tag{5.1}$$

Let us denote $\Omega = (0, 2\pi)^d$ for $d = 2$ or 3. Given an even integer N, we set

$$P_N = \left\{ \phi : \phi(x) = \sum_{k=1}^{N/2} (\tilde{a}_k \cos kx + \tilde{b}_k \sin kx) \right\}, \tag{5.2}$$

and $x_j = \frac{2\pi j}{N}$, $j = 0, 1, \cdots, N-1$.

We also define the discrete inner product P_N as

$$(\phi, \psi)_N = \frac{2\pi}{N} \sum_{j=0}^{N-1} \phi(x_j)\psi(x_j), \tag{5.3}$$

and the corresponding discrete norm by $\|\phi\|_N = \sqrt{(\phi, \phi)_N}$. We recall that the above quadrature rule is exact for $\phi, \psi \in P_{2N}$, *i.e.*,

$$(\phi, \psi)_N = (\phi, \psi), \quad \forall \phi, \psi \in P_{2N}, \tag{5.4}$$

and consequently,

$$\|\phi\|^2 = (\phi, \phi)_N, \quad \forall \phi \in P_N. \tag{5.5}$$

In the multidimensional case, $\Omega = (0, \pi)^d$, we denote $x_{\mathbf{j}} = \Pi_{k=1}^d x_{j_k}$ with $0 \le j_k \le N-1$, $P_{\mathbf{N}} = \Pi_{k=1}^d P_N$, and

$$(\phi, \psi)_{\mathbf{N}} = (\frac{2\pi}{N})^d \sum_{k=1}^{d} \sum_{j_k=0}^{N-1} \phi(x_{j_k})\psi(x_{j_k}). \tag{5.6}$$

With the above notations, we can now write our Fourier-Galerkin method with numerical integration for the scheme (5.1) as follows:

Find $\phi_N^{n+1} \in P_{\mathbf{N}}$ such that

$$\begin{aligned} (\frac{\phi_N^{n+1} - \phi_N^n}{k}, \psi) = &-\frac{1}{4}\left((|\nabla\phi_N^{n+1}|^2 + |\nabla\phi^n|^2)(\nabla\phi_N^{n+1} + \nabla\phi_N^n), \nabla\psi\right)_{\mathbf{N}} \\ &+ (\nabla(\frac{3}{2}\phi_N^n - \frac{1}{2}\phi_N^{n-1}), \nabla\psi) - \frac{\epsilon^2}{2}(\Delta(\phi_N^{n+1} + \phi_N^n), \Delta\psi), \quad \forall \psi \in P_{\mathbf{N}}. \end{aligned} \tag{5.7}$$

Using the same argument as in the proof of Theorem 2, we can prove the following results:

Corollary 1. *The scheme (5.7) is second-order accurate in time, uniquely solvable, and unconditionally energy stable in the sense that*

$$\begin{aligned} E_N(\phi_N^{n+1}) + \frac{1}{4}\|\nabla(\phi_N^{n+1} - \phi_N^n)\|^2 + \frac{\|\phi_N^{n+1} - \phi_N^n\|^2}{k} + \frac{1}{4}\|\nabla(\phi_N^{n+1} + \phi_N^{n-1} - 2\phi_N^n)\|^2 \\ = E_N(\phi_N^n) + \frac{1}{4}\|\nabla(\phi_N^n - \phi_N^{n-1})\|^2, \end{aligned} \tag{5.8}$$

where

$$E_N(\phi) = \frac{1}{4}\|(|\nabla\phi|^2 - 1)\|_N^2 + \frac{\epsilon^2}{2}\|\Delta\phi\|^2.$$

We observe that the weak formulation (5.7) can be intepreted as a Fourier-collocation method thanks to the exactness of the quadrature (5.4). To this end, we introduce the Lagrange functions $\psi_j(x) \in P_N$ such

that $\psi_j(x_k) = \delta_{kj}$ for all $0 \le k, j \le N-1$, and denote by D_N the derivative matrix with $(D_N)_{jl} := \psi_l'(x_j)$. It is shown (see, for example, [**?**]) that

$$(D_N)_{jl} = \begin{cases} \frac{1}{2}(-1)^{j+l} \cot \frac{(j-l)\pi}{N}, & j \neq l, \\ 0, & j = l. \end{cases} \tag{5.9}$$

Therefore, for $\phi \in P_N$, we have $\phi'(x_j) = \sum_{k=0}^{N-1} (D_N)_{jk} \phi(x_k)$. In the multidimensional case, it is clear that, for $\phi \in P_{\mathbf{N}}$, $(\nabla\phi)(x_{\mathbf{j}})$ can be expressed by using the one-dimensional derivative matrix D_N. We can then denote $(\nabla\phi)(x_{\mathbf{j}}) = (\nabla_{\mathbf{N}}\phi)_{\mathbf{j}}$, where $\nabla_{\mathbf{N}}$ is the multidimensional derivative matrix. Similarly, we denote $(\Delta\phi)(x_{\mathbf{j}}) = (\Delta_{\mathbf{N}}\phi)_{\mathbf{j}}$.

Now, it is easy to check that the scheme (5.7) is equivalent to the following Fourier-collocation method:

$$\begin{aligned} \frac{\phi_N^{n+1} - \phi_N^n}{k} = & \frac{1}{4}\nabla_{\mathbf{N}} \cdot \left((|\nabla_N \phi_N^{n+1}|^2 + |\nabla_N \phi^n|^2)(\nabla_{\mathbf{N}}\phi_N^{n+1} + \nabla_{\mathbf{N}}\phi_N^n) \right) \\ & -\nabla_{\mathbf{N}}(\frac{3}{2}\phi_N^n - \frac{1}{2}\phi_N^{n-1}) - \frac{\epsilon^2}{2}\Delta_{\mathbf{N}}^2(\phi_N^{n+1} + \phi_N^n), \end{aligned} \tag{5.10}$$

where, with a slight abuse of notation, ϕ_N^n are vectors with entries being the values of ϕ_N^n at the collocation points $\{x_{\mathbf{j}} : 0 \le j_k \le N-1, k = 1, \cdots, d\}$.

5.3. Finite difference method. The purpose of this section is to define finite difference versions of the schemes (4.4) and (4.5) for the slope selection equation

$$\partial_t \phi = \nabla \cdot \left(|\nabla\phi|^2 \nabla\phi \right) - \Delta\phi - \epsilon^2 \Delta^2 \phi \ . \tag{5.11}$$

Let $\Omega = (0, L_x) \times (0, L_y)$, where $L_x = m_x \cdot h$ and $L_y = m_y \cdot h$, where $h > 0$. Set $p_i = (i - 1/2) \cdot h$ for i taking integer and half-integer values. Let $E_{m_x} = \{p_i \,|\, i = -1/2, 3/2, \ldots, m_x + 1/2\}$ and similarly for E_{m_y}. Define $C_{m_x} = \{p_i \,|\, i = 1, 2, \ldots, m_x\}$, $C_{m_x}^+ = C_{m_x} \cup \{x_0, x_{m_x+1}\}$, and similarly for C_{m_y} and $C_{m_y}^+$. We define the following 2D grid-function spaces:

$$\mathcal{V}_{m_x \times m_y} = \left\{ u : E_{m_x} \times E_{m_y} \to \mathbb{R} \right\} \ , \tag{5.12}$$

$$\mathcal{C}_{m_x \times m_y} = \left\{ \phi : C_{m_x} \times C_{m_y} \to \mathbb{R} \right\} \ , \quad \mathcal{C}^+_{m_x \times m_y} = \left\{ \phi : C^+_{m_x} \times C^+_{m_y} \to \mathbb{R} \right\}, \tag{5.13}$$

$$\mathcal{E}^{\mathrm{ew}}_{m_x \times m_y} = \left\{ f : E_{m_x} \times C_{m_y} \to \mathbb{R} \right\} \ , \quad \mathcal{E}^{\mathrm{ns}}_{m_x \times m_y} = \left\{ f : C_{m_x} \times E_{m_y} \to \mathbb{R} \right\} \ . \tag{5.14}$$

The functions of $\mathcal{V}_{m_x \times m_y}$ are identified via $u_{i+1/2, j+1/2} := u(p_{i+1/2}, p_{j+1/2})$; those of $\mathcal{C}_{m_x \times m_y}$ and $\mathcal{C}^+_{m_x \times m_y}$ are identified via $\phi_{i,j} := \phi(p_i, p_j)$; those of $\mathcal{E}^{\mathrm{ew}}_{m_x \times m_y}$ are identified via $f_{i+1/2, j} := f(p_{i+1/2}, p_j)$; and, finally, those of $\mathcal{E}^{\mathrm{ns}}_{m_x \times m_y}$ are identified via $f_{i, j+1/2} := f(p_i, p_{j+1/2})$.

We define the operator $d_x : \mathcal{E}^{\mathrm{ew}}_{m_x \times m_y} \to \mathcal{C}_{m_x \times m_y}$ component-wise via

$$d_x f_{i,j} = \frac{1}{h} \left(f_{i+1/2, j} - f_{i-1/2, j} \right) \ , \ {\scriptstyle i=1,\ldots,m_x \atop j=1,\ldots,m_y} \ , \tag{5.15}$$

and define $D_x : \mathcal{C}^+_{m_x \times m_y} \to \mathcal{E}^{\mathrm{ew}}_{m_x \times m_y}$ component-wise via

$$D_x \phi_{i+1/2, j} = \frac{1}{h} \left(\phi_{i+1, j} - \phi_{i,j} \right) \ , \ {\scriptstyle i=0,\ldots,m_x \atop j=1,\ldots,m_y} \ . \tag{5.16}$$

The operators $d_y : \mathcal{E}^{\mathrm{ns}}_{m_x \times m_y} \to \mathcal{C}_{m_x \times m_y}$ and $D_y : \mathcal{C}^+_{m_x \times m_y} \to \mathcal{E}^{\mathrm{ns}}_{m_x \times m_y}$ are defined analogously. The standard 2D discrete Laplacian, $\Delta_h : \mathcal{C}^+_{m_x \times m_y} \to \mathcal{C}_{m_x \times m_y}$, is defined as

$$\Delta_h \phi_{i,j} = d_x(D_x\phi)_{i,j} + d_y(D_y\phi)_{i,j} = \frac{1}{h^2} \left(\phi_{i+1,j} + \phi_{i-1,j} + \phi_{i,j+1} + \phi_{i,j-1} - 4\phi_{i,j} \right), \ {\scriptstyle i=1,\ldots,m_x \atop j=1,\ldots,m_y} \ . \tag{5.17}$$

Define the center-to-vertex derivatives $\mathfrak{D}_x$, $\mathfrak{D}_y : \mathcal{C}^+_{m_x\times m_y} \to \mathcal{V}_{m_x\times m_y}$ component-wise as

$$\mathfrak{D}_x\phi_{i+1/2,j+1/2} := \frac{1}{2h}\left(\phi_{i+1,j+1} - \phi_{i,j+1} + \phi_{i+1,j} - \phi_{i,j}\right) \ , \ {}^{i=0,\dots,m_x}_{j=0,\dots,m_y} \ , \tag{5.18}$$

$$\mathfrak{D}_y\phi_{i+1/2,j+1/2} := \frac{1}{2h}\left(\phi_{i+1,j+1} - \phi_{i+1,j} + \phi_{i,j+1} - \phi_{i,j}\right) \ , \ {}^{i=0,\dots,m_x}_{j=0,\dots,m_y} \ . \tag{5.19}$$

The utility of these definitions is that the differences $\mathfrak{D}_x$ and $\mathfrak{D}_y$ are collocated on the grid, unlike the case for D_x, D_y. Define the vertex-to-center derivatives $\mathfrak{d}_x$, $\mathfrak{d}_y : \mathcal{V}_{m_x\times m_y} \to \mathcal{C}_{m_x\times m_y}$ component-wise as

$$\mathfrak{d}_x u_{i,j} := \frac{1}{2h}\left(u_{i+1/2,j+1/2} - u_{i-1/2,j+1/2} + u_{i+1/2,j-1/2} - u_{i-1/2,j-1/2}\right) , \ {}^{i=1,\dots,m_x}_{j=1,\dots,m_y} \ , \tag{5.20}$$

$$\mathfrak{d}_y u_{i,j} := \frac{1}{2h}\left(u_{i+1/2,j+1/2} - u_{i+1/2,j-1/2} + u_{i-1/2,j+1/2} - u_{i-1/2,j-1/2}\right) , \ {}^{i=1,\dots,m_x}_{j=1,\dots,m_y} \ . \tag{5.21}$$

We say the cell-centered function $\phi \in \mathcal{C}^+_{m_x\times m_y}$ is periodic if and only if

$$\phi_{m+1,j} = \phi_{1,j}, \quad \phi_{0,j} = \phi_{m,j}, \quad j = 1,\dots,m_y, \tag{5.22}$$

$$\phi_{i,n+1} = \phi_{i,1}, \quad \phi_{i,0} = \phi_{i,n}, \quad i = 0,\dots,m_x+1. \tag{5.23}$$

A similar notion exists for grid functions from $\mathcal{V}_{m_x\times m_y}$, $\mathcal{E}^{\rm ew}_{m_x\times m_y}$, and $\mathcal{E}^{\rm ns}_{m_x\times m_y}$ as well.

The first-order convex-splitting, finite difference scheme for the slope selection equation (5.11) scheme that was used (though not described) in [28] is the following: given $\phi^n \in \mathcal{C}^+_{m_x\times m_y}$ periodic, find $\phi^{n+1} \in \mathcal{C}^+_{m_x\times m_y}$ periodic such that

$$\phi^{n+1} - k\left[\mathfrak{d}_x\left\{r^{n+1}\mathfrak{D}_x\phi^{n+1}\right\} + \mathfrak{d}_y\left\{r^{n+1}\mathfrak{D}_y\phi^{n+1}\right\}\right] + k\epsilon^2\Delta_h w^{n+1} = \phi^n - k\Delta\phi^n \ , \tag{5.24}$$

where $r^{n+1} := \left(\mathfrak{D}_x\phi^{n+1}\right)^2 + \left(\mathfrak{D}_y\phi^{n+1}\right)^2 \in \mathcal{V}_{m_x\times m_y}$, and $w^{n+1} := \Delta_h\phi^{n+1} \in \mathcal{C}^+_{m_x\times m_y}$ is periodic. The finite difference version of the compact scheme (4.5) is precisely: given ϕ^{n-1}, ϕ^n, $w^n \in \mathcal{C}^+_{m_x\times m_y}$ periodic, find $\phi^{n+1} \in \mathcal{C}^+_{m_x\times m_y}$ periodic such that

$$\begin{aligned}\phi^{n+1} - \frac{k}{4}\left[\mathfrak{d}_x\left\{\left(r^{n+1}+r^n\right)\left(\mathfrak{D}_x\phi^{n+1}+\mathfrak{D}_x\phi^n\right)\right\} + \mathfrak{d}_y\left\{\left(r^{n+1}+r^n\right)\left(\mathfrak{D}_y\phi^{n+1}+\mathfrak{D}_y\phi^n\right)\right\}\right] \\ + \frac{k\epsilon^2}{2}\left(\Delta_h w^{n+1} + \Delta_h w^n\right) = \phi^n - k\left(\frac{3}{2}\Delta_h\phi^n - \frac{1}{2}\Delta_h\phi^{n-1}\right) \ ,\end{aligned} \tag{5.25}$$

where w^{n+1} is periodic. Finally, the second-order finite difference version of (4.4) is as follows: given ϕ^{n-1}, ϕ^n, $w^n \in \mathcal{C}^+_{m_x\times m_y}$ periodic, find $\phi^{n+1} \in \mathcal{C}^+_{m_x\times m_y}$ periodic such that

$$\begin{aligned}\phi^{n+1} &- \frac{k}{4}\left[\mathfrak{d}_x\left\{r^{n+1}\mathfrak{D}_x\phi^{n+1}\right\} + \mathfrak{d}_y\left\{r^{n+1}\mathfrak{D}_y\phi^{n+1}\right\} + \mathfrak{d}_x\left\{r^n\mathfrak{D}_x\phi^n\right\} + \mathfrak{d}_y\left\{r^n\mathfrak{D}_y\phi^n\right\}\right] \\ &- \frac{k}{12}\left[\mathfrak{d}_x\left\{r^{n+1}\mathfrak{D}_x\phi^n\right\} + \mathfrak{d}_y\left\{r^{n+1}\mathfrak{D}_y\phi^n\right\} + \mathfrak{d}_x\left\{r^{n+1}\mathfrak{D}_x\phi^n\right\} + \mathfrak{d}_y\left\{r^{n+1}\mathfrak{D}_y\phi^n\right\}\right] \\ &- \frac{k}{6}\left[\mathfrak{d}_x\left\{\hat{r}^{n+1}\left(\mathfrak{D}_x\phi^{n+1}+\mathfrak{D}_x\phi^n\right)\right\} + \mathfrak{d}_y\left\{\hat{r}^{n+1}\left(\mathfrak{D}_y\phi^{n+1}+\mathfrak{D}_y\phi^n\right)\right\}\right] \\ &+ \frac{k\epsilon^2}{2}\left(\Delta_h w^{n+1} + \Delta_h w^n\right) = \phi^n - k\left(\frac{3}{2}\Delta_h\phi^n - \frac{1}{2}\Delta_h\phi^{n-1}\right) \ ,\end{aligned} \tag{5.26}$$

where $\hat{r}^{n+1} := \mathfrak{D}_x\phi^{n+1}\cdot\mathfrak{D}_x\phi^n + \mathfrak{D}_y\phi^{n+1}\cdot\mathfrak{D}_y\phi^n \in \mathcal{V}_{m_x\times m_y}$, and the other quantities are the same as defined above.

We now define some grid inner-products and norms:

$$(\phi\|\psi) = \sum_{i=1}^{m}\sum_{j=1}^{n}\phi_{i,j}\psi_{i,j}, \quad \phi,\, \psi \in \mathcal{C}_{m_x\times m_y}\cup\mathcal{C}^{+}_{m_x\times m_y}, \tag{5.27}$$

$$\begin{aligned}\langle u\|v\rangle = \frac{1}{4}\sum_{i=1}^{m}\sum_{j=1}^{n}\big(&u_{i+1/2,j+1/2}v_{i+1/2,j+1/2} + u_{i-1/2,j+1/2}v_{i-1/2,j+1/2}\\ &+u_{i+1/2,j-1/2}v_{i+1/2,j-1/2} + u_{i-1/2,j-1/2}v_{i-1/2,j-1/2}\big), \quad u,\, v \in \mathcal{V}_{m_x\times m_y},\end{aligned} \tag{5.28}$$

$$[f\|g]_{\mathrm{ew}} = \frac{1}{2}\sum_{i=1}^{m}\sum_{j=1}^{n}\left(f_{i+1/2,j}g_{i+1/2,j} + f_{i-1/2,j}g_{i-1/2,j}\right), \quad f,\, g \in \mathcal{E}^{\mathrm{ew}}_{m_x\times m_y}, \tag{5.29}$$

$$[f\|g]_{\mathrm{ns}} = \frac{1}{2}\sum_{i=1}^{m}\sum_{j=1}^{n}\left(f_{i,j+1/2}g_{i,j+1/2} + f_{i,j-1/2}g_{i,j-1/2}\right), \quad f,\, g \in \mathcal{E}^{\mathrm{ns}}_{m_x\times m_y}. \tag{5.30}$$

If $\phi \in \mathcal{C}_{m_x\times m_y}\cup\mathcal{C}^{+}_{m_x\times m_y}$, then $\|\phi\|_2 := \sqrt{h^2\,(\phi\|\phi)}$, and for all $\phi \in \mathcal{C}^{+}_{m_x\times m_y}$, define

$$\|\nabla_h\phi\|_2 := \sqrt{h^2\,[D_x\phi\|D_x\phi]_{\mathrm{ew}} + h^2\,[D_y\phi\|D_y\phi]_{\mathrm{ns}}}\,. \tag{5.31}$$

We now can establish the following summation-by-parts formulae for periodic grid functions. We omit the proofs for the sake of brevity.

Proposition 1. *Let $\phi \in \mathcal{C}^{+}_{m_x\times m_y}$ and $u \in \mathcal{V}_{m_x\times m_y}$ be periodic grid functions. Then*

$$h^2\,\langle\mathfrak{D}_x\phi\|u\rangle = -h^2\,(\phi\|\mathfrak{d}_x u) \quad \textit{and} \quad h^2\,\langle\mathfrak{D}_y\phi\|u\rangle = -h^2\,(\phi\|\mathfrak{d}_y u)\,. \tag{5.32}$$

If $\phi \in \mathcal{C}^{+}_{m_x\times m_y}$, $f \in \mathcal{E}^{\mathrm{ew}}_{m_x\times m_y}$, and $g \in \mathcal{E}^{\mathrm{ns}}_{m_x\times m_y}$ are periodic grid functions, then

$$h^2\,[D_x\phi\|f]_{\mathrm{ew}} = -h^2\,(\phi\|d_x f) \quad \textit{and} \quad h^2\,[D_y\phi\|f]_{\mathrm{ns}} = -h^2\,(\phi\|d_y f)\,. \tag{5.33}$$

Let $\phi,\, \psi \in \mathcal{C}^{+}_{m_x\times m_y}$ be periodic. Then

$$h^2\,[D_x\phi\|D_x\psi]_{\mathrm{ew}} + h^2\,[D_y\phi\|D_y\psi]_{\mathrm{ns}} = -h^2\,(\phi\|\Delta\psi) \quad \textit{and} \quad h^2\,(\phi\|\Delta\psi) = h^2\,(\Delta\phi\|\psi)\,. \tag{5.34}$$

Now, a discrete energy corresponding to (1.5) may be defined as

$$E_h(\phi) := \frac{h^2}{4}\left\langle\left(\left(\mathfrak{D}_x\phi\right)^2 + \left(\mathfrak{D}_y\phi\right)^2\right)^2 + \mathbf{1}\middle\|\mathbf{1}\right\rangle - \frac{1}{2}\,\|\nabla_h\phi\|_2^2 + \frac{\epsilon^2}{2}\,\|\Delta_h\phi\|_2^2\,, \tag{5.35}$$

for all $\phi \in \mathcal{C}^{+}_{m_x\times m_y}$. Using the summation-by-parts formulae just given, and the techniques for the space continuous case, we can establish the following result:

Corollary 2. *The schemes (5.25) and (5.26) are second-order accurate in time and space and unconditionally stable. More precisely, we find*

$$\begin{aligned}E_h\left(\phi^{n+1}\right) + \frac{1}{4}\left\|\nabla_h(\phi^{n+1}-\phi^n)\right\|_2^2 + \frac{1}{k}\left\|\phi^{n+1}-\phi^n\right\|_2^2 + \frac{1}{4}\left\|\nabla_h\left(\phi^{n+1}+\phi^{n-1}-2\phi^n\right)\right\|_2^2\\ = E_h\left(\phi^n\right) + \frac{1}{4}\left\|\nabla_h\left(\phi^n-\phi^{n-1}\right)\right\|_2^2\,.\end{aligned} \tag{5.36}$$

Both schemes are uniquely solvable. The scheme (5.26) enjoys the additional property that it is the Euler-Lagrange equation for a strictly convex, coercive variation problem (in finite dimensions).

Because of the last fact, solving the scheme (5.26) is equivalent to minimizing a coercive, strictly convex functional, $E_{h,scheme}(\phi)$, at each time step. To compute the results given in the next section we use the simple Polak-Ribiére variant of the nonlinear conjugate gradient method for the minimization step [21]. In our implementation, in contrast to what is usually done (see, *e.g*, [1, 2]), we avoid using Brent's method in the line search stage, since it uses only information about the function to be minimized, namely $E_{h,scheme}(\phi)$. (Note also that, since Brent's method is a comparison method, line minimizers are found with, at best, only single-precision precision accuracy.) In place of Brent's method for line search (that is, line minimization of $E_{h,scheme}(\phi)$) we directly use the gradient information and a secant method to do the line search. In other words, instead of finding a line minimizer, we perform the equivalent operation of finding a line zero of the gradient; and to do the latter we use a simple secant method. This can be expressed as

$$\bar{\alpha} = \text{argmin}_\alpha E_{h,scheme}(\phi + \alpha\zeta) = \text{argzero}_\alpha \left(\delta_\phi E_{h,scheme}(\phi + \alpha\zeta) \| \zeta\right). \tag{5.37}$$

where ζ is a given search direction and $\alpha \in \mathbb{R}$. Setting

$$g(\alpha) := \left(\delta_\phi E_{h,scheme}(\phi + \alpha\zeta) \| \zeta\right), \tag{5.38}$$

we employ the secant search scheme

$$\alpha_{\ell+1} = \alpha_\ell - \frac{g(\alpha_\ell)}{s_\ell}, \quad s_\ell = \frac{g(\alpha_\ell) - g(\alpha_{\ell-1})}{\alpha_\ell - \alpha_{\ell-1}}. \tag{5.39}$$

We have the guaranteed convergence $\lim_{\ell\to\infty} \alpha_\ell = \bar{\alpha}$ due to strict convexity. In this way, we need not ever actually assemble or compute the functional $E_{h,scheme}(\phi)$.

6. Numerical results. In this section we present some computational results for the slope selection equation, *i.e.*, (1.5) – (1.7) or (5.11), using our second-order finite difference scheme (5.26) described in the last section. We use the simple nonlinear conjugate gradient solver just described to solve the algebraic equations at each time step. We first present a numerical test that gives evidence of the expected second-order convergence of the scheme as $h,\, k \to 0$. In a second test, we reproduce some calculations from a previous paper [28] to show that in long-time calculations the scheme predicts the accepted coarsening rates for the system.

As, in [13] we perform a Cauchy-type convergence test of our scheme as $h,\, k \to 0$ along a linear refinement path, namely $k = Ch$. At the final time T, we expect the global error to be $O(k^2) + O(h^2) = O(h^2)$ as $h,\, k \to 0$ along such path. However, the evolution equation (5.11) does not possess a natural time-dependent forcing (or source) term that can be manipulated to give a known solution (although one could be added artificially). So instead of measuring the error, we measure the Cauchy difference, $\delta_\phi(T) := \phi_{h_f}^{N_f} - \phi_{h_c}^{N_c}$, where $h_c = 2h_f$, $k_c = 2k_f$, $T = k_f N_f = k_c N_c$, as $h_c,\, k_c \to 0$. Here ϕ_{h_f} is the finite difference solution obtained using the finer resolution mesh size h_f, and ϕ_{h_c}, the finite difference solution obtained using the coarser resolution mesh size h_c. Using a linear refinement path, we again expect $\|\delta_\phi\|_2 = O(h_c^2)$. Further details of the test can be gleaned from [13]. We use the final time is $T = 0.32$, and the refinement path is taken to be $k = 0.1h$. The other parameters are $\epsilon = 0.1$; $L_x = L_y = 3.2$. The initial data for the test are

$$\phi(x, y, 0) = 0.1 \sin^2\left(\frac{2\pi x}{L_x}\right) \cdot \sin\left(\frac{4\pi(y - 1.4)}{L_y}\right) - 0.1 \cos\left(\frac{2\pi(x - 2.0)}{L_x}\right) \cdot \sin\left(\frac{2\pi y}{L_y}\right). \tag{6.1}$$

The results are given in Tab. 6.1 and give supporting evidence for the expected second-order convergence of the scheme.

We now reproduce a calculation from [28] where we use the scheme to predict the coarsening exponents for the slope selection equation (5.11) on a square domain beginning with random initial data. The results are given in Figs. 6.1 – 6.3. The parameters are $\epsilon = 0.03$ (Figs. 6.1 and 6.2) and $\epsilon = 0.04$ (Fig. 6.3); $L_x = L_y = 12.8$; $h = 12.8/512$; $k = 0.001$, $t \in [0, 400]$; $k = 0.01$, $t \in [4000, 6000]$; and $k = 0.02$, $t \in [6000, 16000]$. Note that the computation in Fig. 6.3 is finished by time $t = 6000$. The pyramid/anti-pyramid shapes of the hills and valleys are evident in Fig. 6.1, and the slopes of the faces of the pyramids are

h_c	h_f	$\|\delta_\phi\|_{L_h^2}$	rate
$1/16$	$1/32$	4.844×10^{-2}	–
$1/32$	$1/64$	1.373×10^{-2}	1.82
$1/64$	$1/128$	3.478×10^{-3}	1.98
$1/128$	$1/256$	8.675×10^{-4}	2.00

TABLE 6.1

L^2 Cauchy convergence test. The final time is $T = 0.32$, and the refinement path is taken to be $k = 0.1h$. The other parameters are $\epsilon = 0.1$; $L_x = L_y = 3.2$. The Cauchy difference is defined via $\delta_\phi := \phi_{h_f} - \phi_{h_c}$, where the approximations are evaluated at time $t = T$. The norm of the Cauchy difference at T is expected to be $\mathcal{O}(k^2) + \mathcal{O}\left(h^2\right) = \mathcal{O}\left(h^2\right)$, and this is confirmed in the test.

approximately 1. The system depicted in Fig. 6.1 clearly saturates (to a one-hill-one-valley configuration) by time 16000. (A similar one-hill-one-valley configuration represents the equilibrium state for $\epsilon = 0.04$ as well, though this is not shown.) Roughly speaking, the saturation time can be gleaned from Fig. 6.2 (or Fig. 6.3 for the $\epsilon = 0.04$ case) as the time after which the roughness and energy are essentially flat. There are ways, as we discuss in [3], that one can use a linear extrapolation of the early-time data to obtain a cheap approximation of the saturation time. Basically, one uses the fact that $E_{\min}(\epsilon) = O(\epsilon)$, though we do not pursue this topic here. We do point out that our calculations here yield

$$\frac{E_{\min}(\epsilon = 0.03)}{E_{\min}(\epsilon = 0.04)} \approx 0.7469 \ , \tag{6.2}$$

which confirms the linear dependence of $E_{\min}$ on ϵ.

The theoretical coarsening exponents for the slope selection equation (as determined by formal scaling arguments) are $\alpha = 1/3$ and $\beta = -1/3$, where the roughness, *i.e.*,

$$w(t) = \sqrt{\frac{1}{|\Omega|}\int_\Omega \left|\phi(\mathbf{x},t) - \bar{\phi}(t)\right|^2 \mathrm{d}\mathbf{x}} \ , \tag{6.3}$$

evolves like $w(t) \sim O(t^\alpha)$, and the energy (1.5) evolves like $E(t) \sim O(t^\beta)$ [18]. (In fact, there is a sense in which these exponents may be established rigorously [16], though we do not need that level of detail here.) In Figs. 6.2 and 6.3 we found the linear least-squares fit of the $\log - \log$ data up to time $t = 100$. Using these fits, for $\epsilon = 0.03$ (Fig. 6.2) we calculate $\alpha \approx 0.3218$ and $\beta \approx -0.3042$, and for $\epsilon = 0.04$ (Fig. 6.3) we calculate $\alpha \approx 0.2997$ and $\beta \approx -0.2918$. Thus we observe that the coarsening exponents are reasonably-well-approximated in our simulations, and our figures agree with those found previously in [28]. This is also in accordance with earlier works [20, 25, 26, 30] although we have computed to longer time horizon (up to steady state) which leads to the "non-straight" part of the coarsening curve.

7. Conclusion remarks. We have presented and analyzed several second order in time, uniquely solvable, unconditionally energy stable, and convergent schemes for gradient flows with Ehrlich-Schwoebel type energy. Applications to models for thin film epitaxial growth with or without slope selection are presented. There are two types of schemes: one type preserves the variational structure of the continuous in time gradient flow while the other doesn't. The ones without variational structure are usually more compact than the ones with variational structure. Fully discretized schemes with either Galerkin Fourier-spectral or Fourier-Galerkin with numerical integration or finite difference in space are also presented and investigated. These fully discrete schemes inherit the same desirable properties as their semi-discrete in time counterparts, including 2nd order in time, unique solvability and unconditional energy stability. We believe that the same methodology may be applied to more general energy functional.

Numerical experiments based on the scheme with variational structure and finite difference in space are conducted on the model with slope selection. Our numerical results verifies the 2nd order accuracy as well as physical coarsening rates of the system.

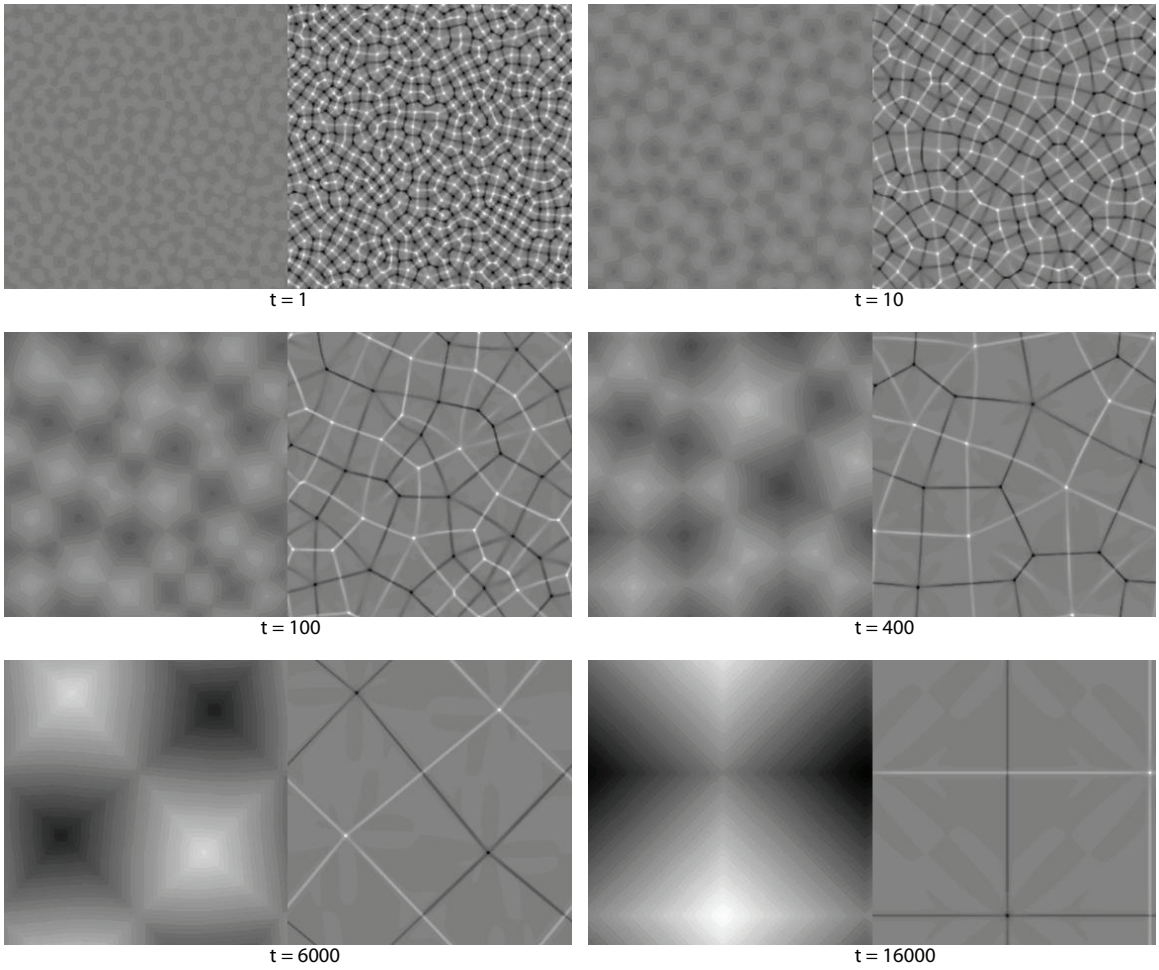

FIG. 6.1. *Time snapshots of the evolution of the model with slope selection. The parameters are* $\epsilon = 0.03$*;* $L_x = L_y = 12.8$*;* $h = 12.8/512$*;* $k = 0.001$*,* $t \in [0, 400]$*;* $k = 0.01$*,* $t \in [4000, 6000]$*; and* $k = 0.02$*,* $t \in [6000, 16000]$*. The left-hand-sides of the snapshots show the filled contour plot of* ϕ*; the right-hand-sides, the filled contour plot of* $\Delta\phi$*. The latter gives an indication of the curvature of the surface* $z = \phi(x, y)$*. The pyramid/anti-pyramid shapes of the hills and valleys are evident in the plots. The system clearly saturates (to a one-hill-one-valley configuration) by time 16000.*

It is still not clear if the scheme proposed here possesses a discrete energy law for general concave (not just quadratic) energy density. A positive answer would be useful since there exists splitting of the Ehrlich-Schwoebel energy with quadratic convex part and non-quadratic concave part for the case without slope selection. If general concave part can be treated explicitly, we will have second order linear scheme that is unconditionally energy stable for thin film epitaxy in the case without slope selection. This would be a nice extension of a result on first order linear scheme that are unconditionally energy stable for the case without slope selection [3].

Acknowledgments. Part of the work was carried out while JS and XW were visiting the Institute for Mathematics and its Applications at the University of Minnesota in the spring of 2010. The financial support and warm hospitality of the Institute are gratefully acknowledged. This work is also supported in part by grants from NSF: DMS-0915066 (JS), DCNS-0959382 (CW), DMS-0606671 and 1008852(XW), and DMS-0818030 (SMW); grants from AFOSR FA9550-08-1-0416 (JS), and 10418149 (CW); and a grant from the Chinese MOE through the 111 project of Modern Applied Mathematics at Fudan University (XW).

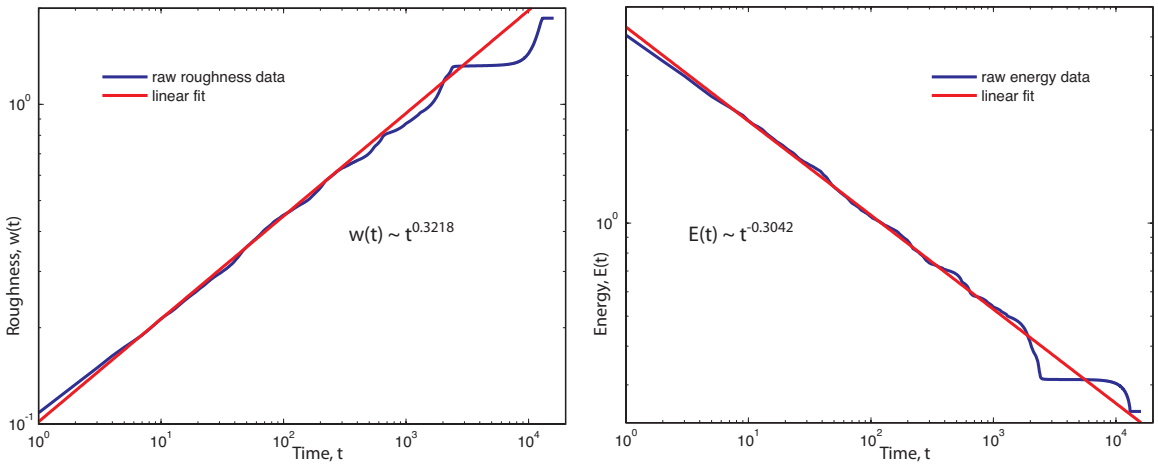

FIG. 6.2. *Roughness and energy evolution for the simulation depicted in Fig. 6.1. The final simulation time is* $T = 16000$. *The theoretical coarsening exponents are* $\alpha = 1/3$ *and* $\beta = -1/3$, *where the roughness evolves like* $w(t) \sim t^{\alpha}$, *and the energy, like* $E(t) \sim t^{\beta}$. *These exponents are reasonably-well-approximated in the simulations.*

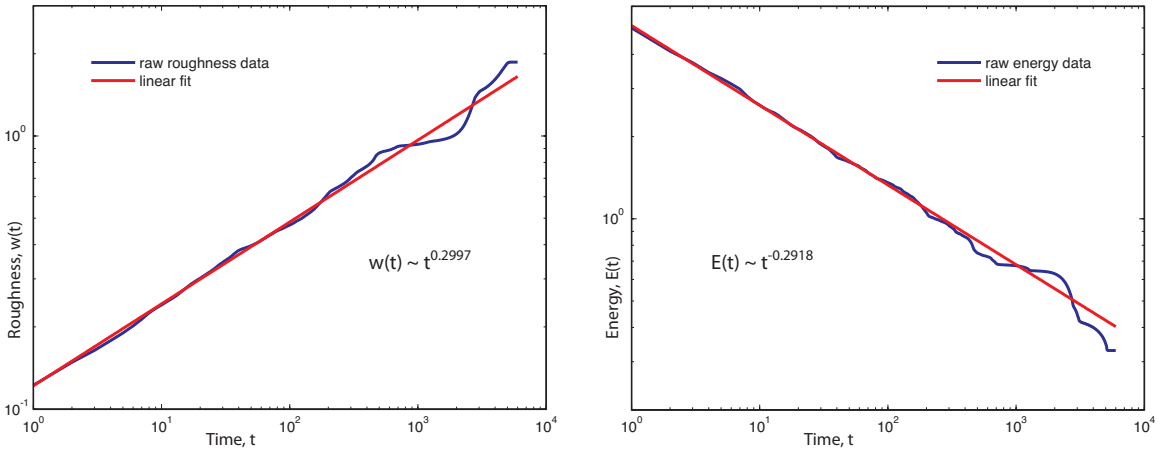

FIG. 6.3. *Roughness and energy evolution for* $\epsilon = 0.04$. *The final simulation time is* $T = 2300$. *All other parameters are the same as in Figs. 6.1 and 6.2. The theoretical coarsening exponents* $\alpha = 1/3$ *and* $\beta = -1/3$ *are reasonably-well-approximated in the simulations.*

REFERENCES

[1] Barrett, J.W. and Liu, W.B.; *Finite element approximation of the p-Laplacian.* MATH. COMP., vol. 61, (1993), pp. 523-537.

[2] Barrett, J.W. and Liu, W.B.; *Finite element approximation of the parabolic p-Laplacian.* SIAM J. NUMER. ANAL., vol. 31, (1994), pp. 413-428.

[3] Chen, W.B.; Conde, S.; Wang, C.; Wang, X. and Wise, S.; *A linear energy stable numerical scheme for epitaxial thin film growth model without slope selection.* submitted to J. SCI. COMP., 2010.

[4] Cheng, M., and Warren, J.A., *An efficient algorithm for solving the phase field crystal model.* J. COMPUT. PHYS., 227:6241, 2008.

[5] Du, Q., Nicolaides, R., *Numerical analysis of a continuum model of a phase transition*, SIAM J. NUM. ANAL., 28, (1991), pp. 1310-1322.

[6] Ekeland, I. and Témam, R.; *Convex analysis and variational problems*, Society for Industrial and Applied Mathematics, c1999.

[7] Ehrlich, G. and Hudda, F.G.; *Atomic view of surface diffusion: Tungsten on tungsten.* J. CHEM. PHYS., 44:1036, 1966.

[8] Evans, J.W. and Thiel, P.A.; *A Little Chemistry Helps the Big Get Bigger.* SCIENCE, 29 October 2010 330: 599-600 DOI: 10.1126/science.1191665

[9] Evans, J.W., Thiel, P.A., and Bartelt, M.C.; *Morphological evolution during epitaxial thin film growth: Formation of 2D islands and 3D mounds*, Surface Science Reports 61 (2006) 1128.
[10] Evans, L.C.; *Partial Differential Equations*. Amer. Math. Soc., Providence, Rhode Island, 1998.
[11] Eyre, D.J.; *Computational and mathematical models of microstructural evolution*, edited by J.W. Bullard et al. (Materials Research Society, Warrendale, PA, 1998), pp. 39-46.
[12] Giaquinta, M.; *Multiple Integrals in the Calculus of Variations and Nonlinear Elliptic Systems*. Princeton Univ. Press, 1983.
[13] Hu, Z., Wise, S.M., Wang, C. and Lowengrub, J.S.; *Stable and efficient finite-difference nonlinear-multigrid schemes for the Phase Field Crystal equation*, J. Comput. Phys., 228, (2009) 5323-5339.
[14] Kohn, R.V.; *Energy-driven pattern formation*. in Proceedings of the International Congress of Mathematicians, Madrid, Spain 2006.
[15] Kohn, R.V. and Otto, F., *Upper bounds on coarsening rates*. Comm. Math. Phys., 229(3):375-395, 2002.
[16] Kohn, R.V. and Yan, X.; *Upper bound on the coarsening rate for an epitaxial growth model*. Comm. Pure Appl. Math., vol. LVI, 1549-1564, (2003).
[17] Li, B.; *High-order surface relaxation versus the Ehrlich-Schwoebel effect*, Nonlinearity, 19 (2006), 25812603.
[18] Li, B. and Liu, J.-G.; *Thin film epitaxy with or without slope selection*. Euro. Jnl of Applied Math. (2003), vol. 14, pp.713-743.
[19] Li, B. and Liu, J.-G.; *Epitaxial growth without slope selection: energetics, coarsening, and dynamic scaling*, J. Nonlinear Sci.. vol. 14, pp. 429-451, (2004).
[20] Moldovan, D. and Golubovic, L,; *Interfacial coarsening dynamics in epitaxial growth with slope selection*, Phys. Rev. E (3), 61 (2000), pp. 61906214.
[21] Polak, E. and Ribiére, G.; *Note sur la convergence des Méthodes de directions conjuguées*. Rev. Fr. Imform. Rech. Oper., vol. 16, (1969), pp. 35-43.
[22] Schwoebel, R.L., *Step motion on crystal surfaces: II*. J. Appl. Phys. 40:614, 1969.
[23] Shen, J. and Yang, X.; *Numerical Approximations of Allen-Cahn and Cahn-Hilliard Equations*, DCDS, Series A, 28:1669-1691 (2010).
[24] Shen, J. and Yang, X., *A phase-field model and its numerical approximation for two-phase incompressible flows with different densities and viscosities*. SIAM J. Sci. Comput., 32:1159-1179 (2010).
[25] Siegert, M.; *Ordering dynamics of surfaces in molecular beam epitaxy*, Phys. A, 239 (1997), pp. 420427.
[26] Siegert, M. and Plischke, M.; *Slope selection and coarsening in molecular beam epitaxy*, Phys. Rev. Lett., 73 (1994), pp. 15171520.
[27] Vollmayr-Lee, B. P. and Rutenberg, A.D.; *Fast and accurate coarsening simulation with an unconditionally stable time step*. Physical Rev. E. 68, 066703 (2003).
[28] Wang, C., Wang, X., and Wise, S., *Unconditionally stable schemes for equations of thin film epitaxy*, Disc. Cont. Dyn. Sys. A vol.28, 2010, pp.405-423.
[29] Wise, S.M., Wang, C. and Lowengrub, J.; *An energy stable and convergent finite-difference scheme for the Phase Field Crystal equation*, SIAM J. Numer. Anal., 47, (2009) 2269-2288.
[30] Xu, C and Tang, T.; *Stability analysis of large time-stepping methods for epitaxial growth models*, SIAM J. Numer. Anal., 44, (2006) 1759-1779.
[31] Ye, X.; *The Legendre collocation method for the Cahn-Hilliard equation*. J. Comput. Appl. Math., 150:87-108 (2003).